https://doi.org/10.15255/KUI.2024.013
KUI-2/2025
Original scientific paper
Received April 18, 2024
Accepted June 3, 2024

Synthesis and Structural Insight into the Bioactivity of Imines with 1,5-Dimethyl-2-Phenyl-1*H*-Pyrazol-3(2*H*)-One Structural Unit Derived from Phenolic Aldehydes

M. Dizdar,[a*] *A. Topčagić*,[a] *M. Avdić*,[b] *D. Vidic*,[a] and *M. Maksimović*[a]

[a] Faculty of Science, University of Sarajevo, Zmaja od Bosne 33–35, 71 000 Sarajevo, Bosnia and Herzegovina

[b] Department of Genetics and Bioengineering, International Burch University, Francuske revolucije bb, 71 210 Ilidža, Bosnia and Herzegovina

Abstract

This study focuses on the synthesis, characterisation, and bioactivity evaluation of four imines derived from the condensation of 4-aminoantipyrine with different phenolic aldehydes: 3-hydroxybenzaldehyde, 4-hydroxybenzaldehyde, 3,4-dihydroxybenzaldehyde, and 4-hydroxy-3-methoxybenzaldehyde. These compounds were synthesised to explore their potential in various biological activities, including antioxidant, acetylcholinesterase (AChE) inhibitory, and antibacterial activities. Characterisation of these imines by IR, ^{1}H and ^{13}C NMR, HR-ESI-MS, and elemental analysis confirmed their proposed structures. The antioxidant activity of the synthesised compounds was assessed using five different methods, with the imine derived from 3,4-dihydroxybenzaldehyde displaying the highest antioxidant activity, attributed to its catechol arrangement of phenolic groups. Additionally, the AChE-inhibitory activity of these compounds was investigated, revealing that the degree of hydroxylation and the introduction of a methoxy group significantly influenced their inhibitory efficacy. Molecular docking studies highlighted the main interactions between the imines and AChE, identifying the most energetically favourable binding sites. Antibacterial testing against *Staphylococcus aureus*, methicillin-resistant *Staphylococcus aureus*, *Pseudomonas aeruginosa*, and *Escherichia coli* indicated that all compounds exhibited broad antibacterial activities. This comprehensive analysis demonstrates the significant potential of these synthesised imines as bioactive molecules, offering insights into how structural modifications can enhance their biological functions.

Keywords

Synthesis, 1H-pyrazol-3(2H)-one, phenolic aldehydes, in vitro bioactivity, in silico study

1 Introduction

From the aspect of secondary metabolites, phenolic compounds are classified into subgroups depending on the structural details present. One important category includes phenolic aldehydes, which can be classified by the number of C atoms in their basic skeleton, as C_6-C_1 and C_6-C_3 (Fig. 1).[1]

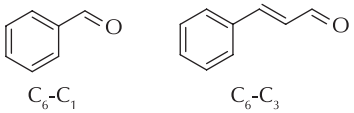

Fig. 1 – Basic skeletons of naturally derived C_6-C_1 and C_6-C_3 phenolic aldehydes

Due to their reactivity and structural diversity, phenolic aldehydes are suitable precursors for synthesising a wide variety of derivatives. The most significant modifications in previous research have been performed on the phenolic, phenyl, and carbonyl groups.[2–4] Often included in more complex structures, the presence of a chiral centre is common, making the process of isolating enantiomerically pure naturally occurring derivatives difficult. On the other hand, in the synthesis of phenolic aldehyde derivatives where the products contain chiral centres, stereo- and regioselective synthesis procedures are frequently applied.[5] Such approaches are necessarily catalysed by chiral catalysts, but also by enzymes, leading to the creation of enantiomerically pure products whose biological activity and receptor binding are conditioned by their stereochemical properties.[6] The most significant modifications in the case of C_6-C_1 phenolic aldehydes involve reactions with the carbonyl group. Interventions in the carbonyl group result in the formation of numerous structurally diverse derivatives, the most significant of which are a large number of heterocycles (piperidin-4-ones, xanthen-1-ones, indoles, *etc.*), synthetic glycosides, coumarins, and many other more complex derivatives.[7–11] The most important and the most investigated derivatives of phenolic aldehydes belong to the class of imines. Namely, this class of derivatives exhibits numerous biological activities, including antimicrobial, anticancer, antiviral, enzyme-inhibitory, and many others. Additionally, imines play a significant role as ligands in the synthesis of transition metal complexes, which often exhibit substantial biological activity, as well as catalytic activity. When combined with 4-aminoantipyrine (AAP), an amine component known for its anti-inflammatory and analgesic activity, numerous imines and metal complexes with

* Corresponding author: Muamer Dizdar, PhD
Email: muamer.dizdar@pmf.unsa.ba

therapeutic effects (such as DNA intercalators, fungicides, antipyretics, *etc.*) have been synthesised.[12–15]

Following this molecular combination strategy, we synthesised four imines derived from substituted benzaldehydes and AAP. Among the synthesised compounds, the imine derived from 3-hydroxybenzaldehyde was synthesised and structurally characterised for the first time. After successful synthesis and structural characterization, all synthesised compounds were tested for antioxidant activity, acetylcholinesterase (AChE) inhibitory activity, and antibacterial activity against four strains. Their efficiency as radical scavengers was evaluated by their reactivity towards the stable 2,2-diphenyl-1-picrylhydrazyl radical (DPPH$^{\bullet}$), 2,2′-azinobis(3-ethylbenzothiazoline-6-sulfonic acid) radical cation (ABTS$^{\bullet+}$), and Oxygen Radical Absorbance Capacity (ORAC). Their reduction power and chelation ability were determined using the Ferric Reducing Antioxidant Power (FRAP) assay and inhibition of Fe(II)-ferrozine complex formation. The *in vitro* Ellman spectrophotometric method was employed to investigate AChE inhibition, while an *in silico* study was conducted to determine the potentially most favourable binding position on AChE. Additionally, antibacterial activity was tested for all synthesised compounds using the agar well method.

2 Experimental

All chemicals were obtained from Sigma-Aldrich and used without further purification. Purification of products was performed by recrystallisation from anhydrous methanol. The purity of the obtained derivatives was evaluated by thin-layer chromatography. Visualisation and detection of the chromatograms was achieved using a UV lamp and 5 % solution of $FeCl_3$. Melting points, uncorrected, were determined using a Kofler apparatus (Reichert Austria). Elemental analysis of the synthesised derivatives was conducted using PerkinElmer CHNS/O Analyzer 2400 Series II. Infrared spectra were recorded using the KBr pellet method in the range of 4000–400 cm^{-1} (PerkinElmer BX FTIR), with bands marked as strong (s), medium (m), or broad (br). Nuclear magnetic resonance (NMR) of ^{1}H and ^{13}C nuclei were recorded in DMSO-d_6 (Bruker AVANCE Ultrashield 500 plus). All shifts in the NMR spectra are reported in ppm (δ) relative to TMS as an internal standard or calibrated against the residual signal of DMSO-d_6 (δ_H q, 2.50; δ_C sept, 39.52). Coupling constants (J) are expressed in Hz. High-resolution mass spectra were recorded using an Agilent 6224 TOF mass spectrometer. All spectrophotometric measurements were performed on a PerkinElmer Lambda 25 UV-Vis.

2.1 Synthesis

The prepared reaction mixture containing an equimolar mixture (2 mmol) of the appropriate aldehyde and AAP, was refluxed in 20 ml of methanol for 4–6 h.[16] The resulting precipitate was vacuum filtered, recrystallised from anhydrous methanol, washed with diethyl ether, and dried under reduced pressure over anhydrous $CaCl_2$. The purity of the imines prepared this way was checked by chromatography on a thin layer of polyamide 11 F_{254} (EtOAc : hexane, 1 : 1).

4-((3-Hydroxybenzylidene)amino)-1,5-dimethyl-2-phenyl-1*H*-pyrazol-3(2*H*)-one (1). White solid; yield: 570 mg, 93 %; R_f 0.43 (EtOAc : hexane, 1 : 1); melting point 132–134 °C; ν/cm^{-1} (KBr): 3431 (m), 3147 (s), 1619 (s), 1591 (s), 1560 (s), 1451 (s), 1286 (s), 1237 (s); ^{1}H NMR (500 MHz, DMSO-d_6) δ_H: 9.56 (s, 1H), 9.49 (s, 1H), 7.57–7.50 (m, 2H), 7.41–7.34 (m, 3H), 7.28–7.22 (m, 2H), 7.19 (dt, J = 7.5, 1.3 Hz, 1H), 6.83 (ddd, J = 8.0, 2.6, 1.1 Hz, 1H), 3.17 (s, 3H), 2.45 (s, 3H); ^{13}C NMR (125 MHz, DMSO-d_6) δ_C: 160.11, 158.13, 155.03, 152.60, 139.39, 135.05, 130.21, 129.61(2), 127.35, 125.04(2), 119.40, 117.96, 116.81, 113.30, 35.84, 10.22; HR-MS (ESI$^+$, m/z): 308.1396 [M+H]$^+$ ($C_{18}H_{18}N_3O_2$ calculated 308.1394); analytically calculated. for $C_{18}H_{17}N_3O_2$: C, 70.34, H, 5.58, N, 13.67, found: C, 70.60, H, 5.68, N, 13.79.

4-((4-Hydroxybenzylidene)amino)-1,5-dimethyl-2-phenyl-1*H*-pyrazol-3(2*H*)-one (2). Yellow solid; yield: 546 mg, 89 %; R_f 0.39 (EtOAc : hexane, 1 : 1); melting point 145–146 °C; ν/cm^{-1} (KBr): 3067 (s), 1654 (s), 1609 (s), 1508 (s), 1274 (s), 1229 (s); ^{1}H NMR (500 MHz, DMSO-d_6) δ_H: 9.91 (s, 1H), 9.48 (s, 1H), 7.68–7.62 (m, 2H), 7.55–7.49 (m, 2H), 7.40–7.32 (m, 3H), 6.88–6.81 (m, 2H), 3.13 (s, 3H), 2.42 (s, 3H); ^{13}C NMR (125 MHz, DMSO-d_6) δ_C: 160.41, 160.13, 155.33, 152.19, 135.23, 129.56(4), 129.32, 127.09, 124.70(2), 117.52, 116.07(2), 36.10, 10.27; HR-MS (ESI$^+$, m/z): 308.1385 [M+H]$^+$ ($C_{18}H_{18}N_3O_2$ calculated 308.1394); analytically calculated for $C_{18}H_{17}N_3O_2$: C, 70.34, H, 5.58, N, 13.67, found: C, 70.56, H, 5.54, N, 13.71.

4-((3,4-Dihydroxybenzylidene)amino)-1,5-dimethyl-2-phenyl-1*H*-pyrazol-3(2*H*)-one (3). Brown solid; yield: 528 mg, 82 %; R_f 0.32 (EtOAc : hexane, 1 : 1); melting point 151–152 °C; ν/cm^{-1} (KBr): 3494 (s), 2946 (m), 1589 (s), 1562 (s), 1449 (s), 1288 (s), 1221 (s); ^{1}H NMR (500 MHz, DMSO-d_6) δ 9.42 (s, 1H), 9.40 (s, 1H), 9.21 (s, 1H), 7.56–7.49 (m, 2H), 7.40–7.33 (m, 3H), 7.32 (d, J = 2.0 Hz, 1H), 7.04 (dd, J = 8.1, 1.9 Hz, 1H), 6.81 (d, J = 8.1 Hz, 1H), 3.13 (s, 3H), 2.42 (s, 3H); ^{13}C NMR (125 MHz, DMSO-d_6) δ_C: 160.43, 155.70, 152.07, 148.66, 146.08, 135.21, 129.82, 129.56(2), 127.08, 124.68(2), 121.34, 117.57, 115.98, 113.41, 36.11, 10.25; HR-MS (ESI$^+$, m/z): 324.1344 [M+H]$^+$ ($C_{18}H_{17}N_3O_3$ calculated 323.1271); analytically calculated for $C_{18}H_{17}N_3O_3$: C, 66.86; H, 5.30; N, 13.00, found: C, 66.53; H, 5.34; N, 12.91.

4-((4-Hydroxy-3-metoxybenzylidene)amino)-1,5-dimethyl-2-phenyl-1*H*-pyrazol-3(2*H*)-one (4). Yellow solid; yield: 596 mg, 88 %; R_f 0.56 (EtOAc : hexane, 1 : 1); melting point 124–125 °C; ν/cm^{-1} (KBr): 3433 (br, w), 3113 (m), 1628 (s), 1581 (s), 1518 (s), 1285 (s), 1258 (s), 1131 (s); ^{1}H NMR (500 MHz, DMSO-d_6) δ_H: 9.52 (s, 1H), 9.47 (s, 1H), 7.56–7.49 (m, 2H), 7.43 (d, J = 2.0 Hz, 1H), 7.41–7.32 (m, 3H), 7.19 (dd, J = 8.1, 1.8 Hz, 1H), 6.85 (d, J = 8.1 Hz, 1H), 3.84 (s, 3H), 3.13 (s, 3H), 2.44 (s, 3H); ^{13}C NMR (125 MHz, DMSO-d_6) δ_C: 160.41, 155.47, 152.21, 149.63, 148.44, 135.24, 129.77, 129.57(2), 127.09, 124.69(2), 122.56, 117.48, 115.90, 109.98, 55.96, 36.11, 10.34; HR-MS (ESI$^+$, m/z): 338.1502 [M+H]$^+$ ($C_{19}H_{19}N_3O_3$ calculated 337.1430); analytically calculated for $C_{19}H_{19}N_3O_3$: C, 67.74; H, 5.68; N, 12.46, found: C, 67.38; H, 5.92; N, 12.13.

2.2 Antioxidant activity

The antioxidant activity was tested using five different methods: DPPH, ABTS, FRAP, ORAC, and Fe(II) chelating ability. Results for the FRAP and ORAC methods are expressed as equivalents of ascorbic acid (AAE) and Trolox (TE), respectively, while for the other methods the results are expressed as IC_{50} values. Ascorbic acid and Trolox were used as standards for all methods involving hydrogen atom (HAT) and single electron transfer (SET) as a key step in the mechanism, whereas Na_2EDTA was the standard for testing chelating properties. For methods where results are expressed in equivalents, calibration curves were constructed based on the standards used. All measurements were performed in triplicate, and the results presented as mean value ± standard deviation.

2.2.1 DPPH method

Antioxidant activity with this method was tested according to the procedure described by Molyneux (2004) with minor modifications.[17] The sample (0.1 ml) was added to 1 ml of a methanol solution of $DPPH^{\bullet}$ (0.08 mM). The obtained mixture was incubated for 30 min in the dark, after which the absorbance was measured at 517 nm.

2.2.2 ABTS method

To test the antioxidant activity using this method, radical cation species were generated by mixing equal volumes of 7 mM ABTS and 2.45 mM $K_2S_2O_8$ solutions and incubating at 4 °C for 16 h.[18] Different concentrations of the tested samples (0.1 ml) were added to 1 ml of the prepared $ABTS^{\bullet+}$ solution, and absorbance was measured after 7 min at 734 nm.

2.2.3 FRAP method

The reduction of Fe^{3+} ions by this method was monitored using the procedure described by *Benzie and Strain*.[19] Stock solutions included 300 mM acetate buffer (pH 3.6), 10 mM 2,4,6-tris(pyridin-2-yl)-*s*-triazine (TPTZ) in ethanol, and 20 mM $FeCl_3$ in 20 mM HCl. To prepare the working FRAP solution, acetate buffer, TPTZ, and $FeCl_3$ solution were mixed in a volume ratio of 10 : 1 : 1 and incubated as such at 37 °C before use. FRAP reagent (3 ml) and 0.3 ml of water were added to an aliquot of the sample (0.1 ml). All measurements were adjusted to 593 nm after 6 min.

2.2.4 ORAC method

Oxygen radical absorption capacity was measured according to the modified procedure described by *Cao et al.*[20] A mixture of 0.05 ml of fluorescein solution (0.42 μM), 0.1 ml of tested sample (1 μM), and 1.8 ml of phosphate buffer (0.1 M, pH 7.3) was incubated at 37 °C for 15 min. After incubation, peroxyl radical formation was initiated by adding 0.05 ml of 2,2′-azobis(2-amidinopropane)dihydrochloride solution (640 mM). All measurements were taken in triplicate, recording fluorescence intensity for 60 min (λ_{ex} 485 nm, λ_{em} 520 nm).

2.2.5 Fe(II) chelating ability

The most important spectrophotometric method for monitoring the chelation of Fe(II) ions is the competitive method of complex formation with ferrozine in the presence of a potential ligand.[21] A 0.05 ml of $FeCl_2$ solution (2 mM) was added to 0.4 ml of the solution of the tested compound. The reaction was initiated by adding 0.2 ml of ferrozine solution (5 mM). The total volume was adjusted to 4 ml with ethanol, mixed, and incubated at room temperature for 10 min. Absorbance was measured at 562 nm.

2.3 AChE inhibition

The potential AChE-inhibitory activity of the synthesised imines was determined using Ellman's method.[22] Galantamine hydrobromide was used as a positive control, while the final concentrations of the tested compounds in the reaction mixture were 0–50 μM. A mixture of 0.3 ml phosphate buffer (100 mM, pH 8.0), 0.3 ml of sample, and 0.3 ml of AChE (0.54 U ml^{-1}) was incubated for 15 min at 37 °C. At the end of incubation, 0.3 ml of acetylcholine iodide (15 mM) and 1.5 ml of 5,5-dithiobis-(2-nitrobenzoic acid) solution (3 mM) were added. For the resulting mixtures, the absorbance was measured at 405 nm for 5 min. A linear equation correlating the common logarithm of the concentration of the tested sample with the percentage of AChE inhibition was used to extrapolate IC_{50} values.

2.4 *In silico* analysis

The structure of synthesised imines was generated using Avogadro, and the geometry was optimised using ORCA software (Neese, 2022). Non-polar hydrogens of imines were merged, and rotatable bonds were defined. The AChE (1C2B) structure was downloaded from the Protein Data Bank.[23] Water molecules were removed, polar hydrogens were added, Kollman united atom partial charges were assigned, and the protein was stored in a separate file for input into AutoDock Tools. Molecular docking was performed using Autodock Vina.[24] The binding sites were defined using grid size coordinates of 60 × 60 × 72, and grid centre coordinates of $x = 21.591$, $y = 87.752$, and $z = 23.591$ with a grid space of 0.375 Å.[25] During the docking process, torsional bonds of the ligand were set free. The protein-ligand complex was visualised and analysed using PyMOL software.[26]

2.5 Antibacterial activity

Agar well method was used to evaluate the antibacterial potential of the synthetic substances.[27] The reference strains that were tested in this study included *Staphylococcus aureus* (ATCC 6538), methicillin-resistant *Staphylococcus aureus* (ATCC 33591), *Pseudomonas aeruginosa* (ATCC 10145), and extended-spectrum beta-lactamase (ESBL) *Escherichia coli* (ATCC 35218). A bacterial inoculum of 0.5 McFarland density was applied to Mueller Hinton agar plates. Wells with a diameter of 8 mm were made in the agar, and 100 μl of the tested compounds (1 mM) was added to each well. Ampicillin was used as a positive standard. Each experiment was conducted in triplicate. Af-

ter overnight incubation at 37 °C, the zones of inhibition were measured and expressed in the form of zones of inhibition measured in mm.

3 Results and discussion

3.1 Synthesis

The target imines (**1–4**) were synthesised by the condensation of AAP with the following aldehydes: 3-hydroxybenzaldehyde, 4-hydroxybenzaldehyde, 3,4-dihydroxybenzaldehyde and 4-hydroxy-3-methoxybenzaldehyde (Fig. 2).

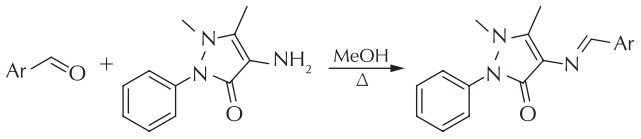

Fig. 2 – Synthesis of compounds **1**–**4**

1 Ar = 3-(OH)C_6H_4, **2** Ar = 4-(OH)C_6H_4,
3 Ar = 3,4-di(OH)C_6H_3, **4** Ar = 4-(OH)-3-(H_3CO)C_6H_3

The most important and extensively studied derivatives of phenolic aldehydes belong to the class of imines.[28,29] This class of derivatives exhibits numerous biological activities, including antimicrobial, anticancer, antiviral, enzyme-inhibitory properties, among others. Additionally, their complex compounds with transition metal complexes frequently show significant biological and catalytic activity. When combined with AAP, an amine component known for its anti-inflammatory and analgesic activity, a large number of imines and metal complexes with therapeutic effects (such as DNA intercalators, fungicides, antipyretics, *etc.*) have been synthesised.[12]

The synthesised imines were characterised by IR, ^{1}H and ^{13}C NMR, HR-ESI-MS, and elemental analysis. All results were consistent with the proposed structures. The purity of the synthesised compounds was, in addition to thin-layer chromatography, checked by elemental analysis, with all compounds having an error margin within ± 0.4 %. Phenolic protons appeared as broad singlets in the range of 9.21–9.91 ppm, while azomethine protons appeared as singlets in the range of 9.40–9.49 ppm in the ^{1}H NMR spectra. In addition to aromatic protons, all compounds showed characteristic singlets of sp^3 methyl protons in the range of 3.17–2.42 ppm, with a characteristic singlet for the methoxy group (3.84 ppm) in the case of imine **3**. Additionally, for all synthesised imines, characteristic peaks were observed in the ^{13}C NMR spectra, and *m*/*z* values for $[M+H]^+$ in HR-ESI-MS spectra.

3.2 Bioactivity

3.2.1 Antioxidant activity

To cover a broad range of mechanisms, all compounds were tested for their ability to reduce and chelate transition metal ions, as well as their ability to neutralize free radicals (Table 1).

The amine component (AAP) possesses no H donor groups that can significantly affect antioxidant activity. Therefore, the free radical reduction/neutralisation ability of these derivatives can be exclusively attributed to the structural details of phenolic aldehydes. A trend of **3**>**4**>**1**≈**2** is noticeable, where the antioxidant capacity of the tested compounds decreases. Such low IC_{50} values and high values of ascorbic acid and Trolox equivalents are most likely due to the double phenolic groups of the catechol arrangement in their structures in the case of compound **3**. The decrease in antioxidant activity in the case of compound **4** can be explained by the additional alkylation of phenolic groups at C_3 positions. Additionally, a significant drop in antioxidant activity is visible for derivatives derived from 3- and 4-hydroxybenzaldehyde, due to the loss of the second substituent on the aromatic nucleus (OH and/or OCH_3). Despite the impossibility of homolytic cleavage, the OCH_3 group in the *ortho* position lowers the oxidation potential, but also acts as an electron-donating group, thereby facilitating the stabilisation of phenoxy radicals.[30] The absence of results for chelation ability is noticeable. Even without the presence of ferrozine, the tested compounds in combination with Fe(II) ions absorbed in the same part of the visible spectrum, making it impossible to test the chelation ability using this method. This behaviour of the imine derivatives might be due to the presence of the AAP unit, known as a ligand in quantitative iron determination procedures,[31] and as a ligand for the synthesis of diverse complex compounds.[32,33]

Table 1 – Antioxidant activity of compounds **1–4**

Compound	DPPH$^{\bullet}$ IC_{50}/μM	$ABTS^{\bullet+}$ IC_{50}/μM	FRAP *AAE* /μmol_{AA}/mmol	ORAC *TE* /μmol_{TE}/μmol
1	105.12 ± 2.45	8.75 ± 0.14	163.55 ± 3.33	0.01 ± 0.00
2	128.63 ± 4.68	10.43 ± 0.29	112.67 ± 2.29	0.02 ± 0.00
3	31.47 ± 0.95	2.04 ± 0.08	405.19 ± 9.11	0.26 ± 0.01
4	47.94 ± 1.02	2.61 ± 0.12	305.37 ± 8.45	0.14 ± 0.00
Ascorbic acid	1.14 ± 0.03	0.11 ± 0.00	–	0.48 ± 0.04

Table 2 – AChE-inhibitory activity of compounds **1–4** and H-bonds in AChE interaction

Compound	IC_{50} / μM	Affinity / kcal mol^{-1}	Bonding in AChE/distance / Å
1	162.72 ± 4.12	−8.7	*H*-Gly^{122} → *O*-[C_3-OH]/2.7 Å
2	163.23 ± 5.78	−7.4	*H*-Gln^{369} → *O*-[C_3-OH]/2.3 Å *H* [C_4-OH] → *O*-Leu^{540}/2.7 Å
3	145.33 ± 2.78	−8.0	*H*-Leu^{289} → *O*-[C_3-OH]/2.5 Å *H* [C_4-OH] → *O*-Leu^{289}/2.7 Å
4	114.07 ± 3.47	−7.3	*H*-His^{287} → *O*-[C_3-OH]/2.4 Å
Galantamine[34]	3.89 ± 0.15	−8.1	*H*-[C_6-OH] → *O*-Arg^{296} / 2.0 Å *H*-Arg^{296} → *O*-[C_6-OH] / 2.2 Å *H*-Phe^{295} → *O*-[C_6-OH] / 2.2 Å

3.2.2 Inhibition of AChE and molecular docking

For all synthesised compounds, the ability to inhibit AChE was tested *in vitro* using Ellman's method, and *in silico* methods were used to find the best interaction positions (Table 2).

A noticeable trend is that the decrease in the degree of hydroxylation and the introduction of a methyl group at position C_3 (compound **4**) leads to an increase in AChE-inhibitory activity. This phenomenon is well-known and is directly correlated with a decrease in hydrophilicity and an increase in the possibility of interaction with non-polar amino acids. On the other hand, varying the positions of the phenolic group at C_3 and C_4, the positions had no significant effect on AChE-inhibitory activity. Additionally, a molecular docking study was conducted to reveal the binding sites and main interactions between the synthesised imine and AChE. Hydrogen bonds were predicted based on the conformation (Fig. 3). These hydrogen bonds form between the amino acid residue of AChE and the

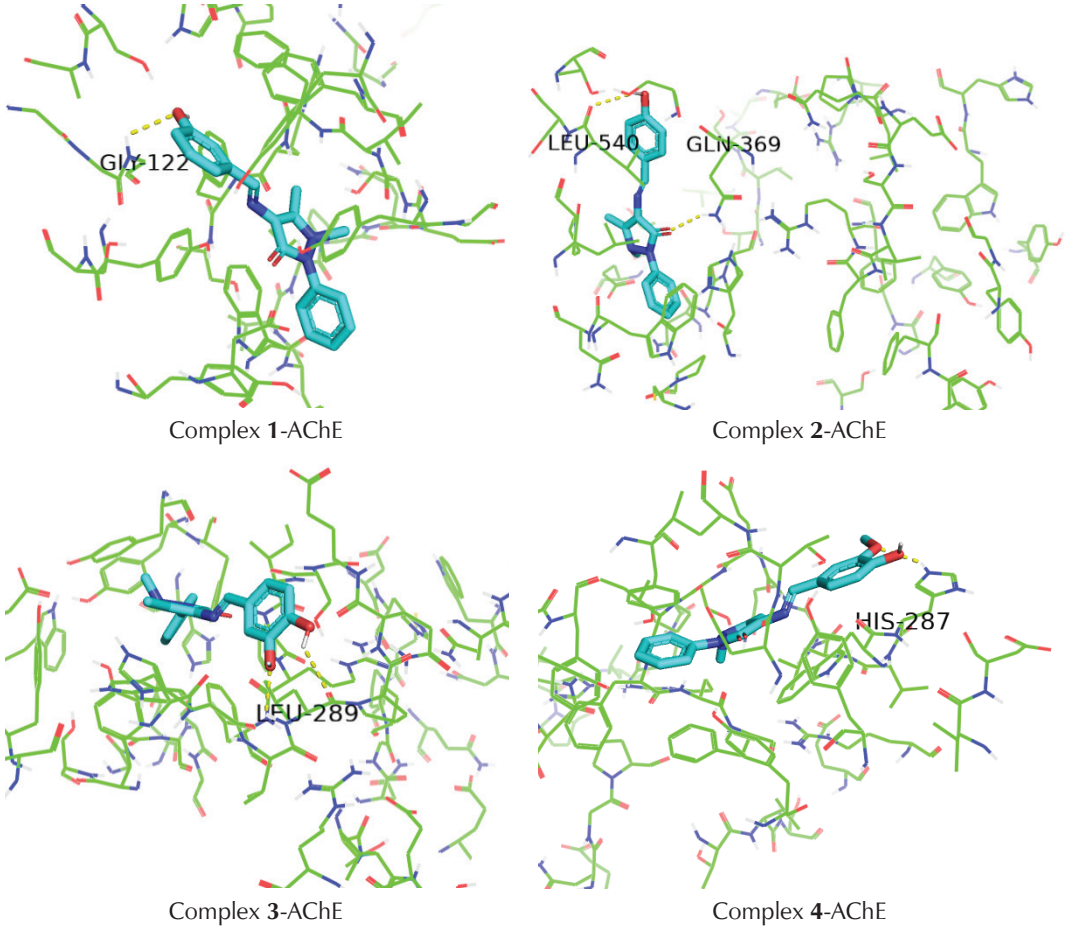

Complex **1**-AChE Complex **2**-AChE

Complex **3**-AChE Complex **4**-AChE

Fig. 3 – Visualisation of favoured binding sites on AChE

Table 3 – Antibacterial activity of compounds **1–4**

Compound	Bacterial strain			
	S. aureus	MRSA	*P. aeruginosa*	ESBL *E. coli*
1	11.00 ± 0.00	–	–	12.00 ± 0.00
2	10.67 ± 0.58	–	–	–
3	10.67 ± 0.58	–	13.00 ± 0.00	11.33 ± 0.58
4	9.33 ± 0.58	–	–	–
Ampicillin	12.33 ± 0.33	–	11.33 ± 0.33	20.67 ± 0.58

oxygen atom of the hydroxyl group on C_3 or the hydrogen atom of the hydroxyl group on C_4 (complexes 2 and 3). The most energetically favourable interaction with AChE showed an estimated docking energy of approximately -8.7 kcal mol^{-1} for compound **1**.

Although there was no significant correlation between the results of *in vitro* and *in silico* analyses, all obtained binding sites have already been reported in numerous studies, and include cases such as coumarins and coumarin-pyrazoles hybrids,[35] pyrazole-pyridazine hybrids,[36] and piperazine derivatives.[37]

3.2.3 Antibacterial evaluations

All synthesised compounds were also tested for antibacterial activity against four strains: *S. aureus*, methicillin-resistant *S. aureus*, *P. aeruginosa,* and ESBL *E. coli* (Table 3).

While compounds **2** and **4**, which have a 4-hydroxy group on the phenolic aldehyde residue, showed antibacterial activity against the Gram-positive *S. aureus*, compounds **1** and **3** also exhibited antibacterial activity against Gram-negative strains. Among these, compound **3** emerged as the best candidate for antibacterial action, demonstrating significant activity against *S. aureus*, *P. aeruginosa*, and ESBL *E. coli*.

4 Conclusion

The synthesised imines **(1-4)** demonstrated significant biological activities, including antibacterial, antioxidative, and AChE-inhibitory activity. These activities are directly associated with the presence of phenolic aldehydes and structural details resulting from condensation with AAP. Notably, compound **3** stood out due to its double phenolic groups, which contributed to its high antioxidative activity. However, variations in hydroxylation and alkylation of phenolic groups showed diverse effects on AChE-inhibitory and antibacterial activity, where variations in the degree of hydroxylation and the presence of a methyl group at position C_3 led to an increase in AChE inhibitory activity. Antibacterial testing revealed that compounds **2** and **4** were active against Gram-positive *S. aureus* strains, while compounds **1** and **3** showed activity against Gram-negative strains, highlighting compound **3** as the best candidate for antibacterial activity. These results suggest that structural variations in imines can be crucial for optimising and targeting specific biological activities. Despite certain limitations, such as the lack of data on chelation ability due to interactions with Fe(II), this research clearly demonstrates the potential of imines derived from phenolic aldehydes as potent biologically active molecules. In conclusion, this study enhances our understanding of the structural and functional relationships in the design of imines with diverse biological activities and paves the way for further research aimed at developing new therapeutic agents.

List of abbreviations

AAE – equivalents of ascorbic acid
AAP – 4-Aminoantipyrine
ABTS – 2,2′-Azinobis(3-ethylbenzothiazoline-6-sulfonic acid)
AChE – Acetylcholinesterase
DPPH$^{\bullet}$ – 2,2-diphenyl-1-picrylhydrazyl radical
ESBL – extended-spectrum beta-lactamase
FRAP – Ferric Reducing Antioxidant Power
ORAC – Oxygen Radical Absorbance Capacity
TE – Trolox

ACKNOWLEDGEMENTS

This work was supported by the Ministry of Education, Science and Youth of the Sarajevo Canton (Grant No. 01/01-1237/4-2023 and 27-02-35-37080-10/23).

References
Literatura

1. *J. Santana-Gálvez, D. A. Jacobo-Velázquez*, Classification of Phenolic Compounds, in *L. M. Nollet, J. A. Gutierrez-Uribe* (eds.), Phenolic compounds in food: Characterization and analysis. CRC Press, Boca Raton, 2017, pp. 1–18.
2. *M. A. Hassan, A. M. Omer, E. Abbas, W. M. Baset, T. M. Tamer*, Preparation, physicochemical characterization and antimicrobial activities of novel two phenolic chitosan Schiff base derivatives, Sci. Rep. **8** (2018) 11416, doi: https://doi.org/10.1038/s41598-018-29650-w.
3. *A. A. Güngör, M. Tümer, M. Köse, S. Erkan*, Benzaldehyde

derivatives with functional propargyl groups as α-glucosidase inhibitors, J. Mol. Struct. **1206** (2020) 127780, doi: https://doi.org/10.1016/j.molstruc.2020.127780.

4. *Y. F. Mustafa, M. K. Bashir, M. K. Oglah*, Original and innovative advances in the synthetic schemes of coumarin-based derivatives: A review, Sys. Rev. Pharm. **11** (2020) 598, doi: https://doi.org/10.5530/srp.2019.2.04.
5. *M. DellaGreca, A. Fiorentin, P. Monaco, L. Previtera*, Enantioselective synthesis of phenylpropanetriols, Synth. Commun. **28** (1998) 3693–3700, doi: https://doi.org/10.1080/00397919808004916.
6. *M. Orlandi, B. Rindone, G. Molteni, P. Rummakko, G. Brunow*, Asymmetric biomimetic oxidations of phenols: the mechanism of the diastereo- and enantioselective synthesis of dehydrodiconiferyl ferulate (DDF) and dehydrodiconiferyl alcohol (DDA), Tetrahedron **57** (2001) 371–378, doi: https://doi.org/10.1016/S0040-4020(00)00944-3.
7. *Y. Eryanti, T. Herlina, A. Zamri, S. N. A. Halim, Y. Shiono, Y. M. Syah, K. Awang, U. Supratman*, 3,5-Bis(2-hydroxybenzylidene)piperidin-4-one, Molbank **2014** (2014) 825, doi: https://doi.org/10.3390/M825.
8. *M. Tajbakhsh, M. Heidary, R. Hosseinzadeh, M. A. Amiri*, $FeCl_3{\cdot}6H_2O$ as a green and readily available catalyst for the synthesis of 1-oxo-hexahydroxanthenes by the condensation of salicylaldehydes with 1,3-diketones in aqueous media, Tetrahedron Lett. **57** (2016) 141–145, doi: https://doi.org/10.1016/j.tetlet.2015.11.088.
9. *Y. Qu, F. Ke, L. Zhou, Z. Li, H. Xiang, D. Wu, X. Zhou*, Synthesis of 3-indole derivatives by copper sulfonato Salen catalyzed three-component reactions in water, Chem. Commun. **47** (2011) 3912–3914, doi: https://doi.org/10.1039/c0cc05695b.
10. *Y. Miyagawa, T. Mizukami, H. Kamitakahara, T. Takano*, Synthesis and fundamental HSQC NMR data of monolignol β-glycosides, dihydromonolignol β-glycosides and *p*-hydroxybenzaldehyde derivative β-glycosides for the analysis of phenyl glycoside type lignin-carbohydrate complexes (LCCs), Holzforschung **68** (2014) 747–760, doi: https://doi.org/10.1515/hf-2013-0164.
11. *P. Verdía, F. Santamarta, E. Tojo*, Knoevenagel Reaction in [MMIm][MSO_4]: Synthesis of Coumarins, Molecules **16** (2011) 4379, doi: https://doi.org/10.3390/molecules16064379.
12. *C. J. Dhanaraj, S. S. Raj*, Synthesis, characterization and biological studies of Schiff base metal complexes derived from 4-aminoantipyrine, acetamide and *p*-phenylenediamine, Inorg. Chem. Commun. **119** (2020) 108087, doi: https://doi.org/10.1016/j.inoche.2020.108087.
13. *R. Teran, R. Guevara, J. Mora, L. Dobronski, O. Barreiro-Costa, T. Beske, J. Pérez-Barrera, R. Araya-Maturana, P. Rojas-Silva, A. Poveda, J. Heredia-Moya*, Characterization of antimicrobial, antioxidant, and leishmanicidal activities of Schiff base derivatives of 4-aminoantipyrine, Molecules **24** (2019) 2696, doi: https://doi.org/10.3390/molecules24152696.
14. *K. Sunand, K. V. Kumar, K. Ashwini, P. Suresh Kumar, S. Vishnu, A. Samala*, Synthesis characterization, antibacterial studies of 4-aminoantipyrine schiff's bases, Int. J. Appl. Pharm. Sci. Res. **2** (2017) 8–14, doi: https://doi.org/10.21477/ijapsr.v2i1.6908.
15. *R. M. Issa, A. M. Khedr, H. F. Rizk*, UV–vis, IR and ^{1}H NMR spectroscopic studies of some Schiff bases derivatives of 4-aminoantipyrine, Spectrochim. Acta A Mol. Biomol. Spectrosc. **62** (2005) 621–629, doi: https://doi.org/10.1016/j.saa.2005.01.026.
16. *A. Jiménez-Sánchez, M. Rodríguez, R. Métivier, G. Ramos-Ortíz, J. L. Maldonado, N. Réboles, N. Farfán, K. Nakatani, R. Santillan*, Synthesis and crystal structures of a series of Schiff bases: a photo-, solvato- and acidochromic compound, New J. Chem. **38** (2014) 730–738, doi: https://doi.org/10.1039/C3NJ00895A.
17. *P. Molyneux*, The use of the stable free radical diphenylpicrylhydrazyl (DPPH) for estimating antioxidant activity, Songklanakarin J. Sci. Technol. **26** (2004) 211–219.
18. *N. A. Abed, M. M. Hammouda, M. A. Ismail, E. Abdel-Latif*, Synthesis of new heterocycles festooned with thiophene and evaluating their antioxidant activity, J. Heterocycl. Chem. **57** (2020) 4153–4163, doi: https://doi.org/10.1002/jhet.4122.
19. *I. F. Benzie, J. J. Strain*, The Ferric Reducing Ability of Plasma (FRAP) as a measure of "antioxidant power": The FRAP assay, Anal. Biochem. **239** (1996) 70–76, doi: https://doi.org/10.1006/abio.1996.0292.
20. *G. Cao, E. Sofic, R. L. Prior*, Antioxidant capacity of tea and common vegetables, J. Agric. Food Chem. **44** (1996) 3426–3431, doi: https://doi.org/10.1021/jf9602535.
21. *D. Dharumadurai*, Methods in Actinobacteriology. Humana Press, New York, USA, 2022, pp. 457–458, doi: https://doi.org/10.1007/978-1-0716-1728-1.
22. *G. L. Ellman, K. D. Courtney, V. Andres jr., R. M. Featherstone*, A new and rapid colorimetric determination of acetylcholinesterase activity, Biochem. Pharmacol. **7** (1961) 88–90, doi: https://doi.org/10.1016/0006-2952(61)90145-9.
23. *Y. Bourne, J. Grassi, P. Bougis, P. Marchot*, Conformational flexibility of the acetylcholinesterase tetramer suggested by X-ray crystallography, J. Biol. Chem. **274** (1999) 30370–30376, doi: https://doi.org/10.1074/jbc.274.43.30370.
24. *O. Trott, A. J. Olson*, AutoDock Vina: Improving the speed and accuracy of docking with a new scoring function, efficient optimization, and multithreading, J. Comput. Chem. **31** (2010) 455–461, doi: https://doi.org/10.1002/jcc.21334.
25. *O. M. Bautista-Aguilera, G. Esteban, I. Bolea, K. Nikolic, D. Agbaba, I. Moraleda, I. Iriepa, A. Samadi, E. Soriano, M. Unzeta, J. Marco-Contelles*, Design, synthesis, pharmacological evaluation, QSAR analysis, molecular modeling and ADMET of novel donepezil–indolyl hybrids as multipotent cholinesterase/monoamine oxidase inhibitors for the potential treatment of Alzheimer's disease, Eur. J. Med. Chem. **75** (2014) 82–95, doi: https://doi.org/10.1016/j.ejmech.2013.12.028.
26. *W. L. DeLano*, Pymol: An open-source molecular graphics tool, CCP4 Newsl. Protein Crystallogr. **40** (2002) 82–92.
27. *S. K. Sen, M. R. Munshi, A. Kumar, A. A. Mortuza, M. S. Manir, M. A. Islam, M. N. Hossain, M. Khalid Hossain*, Structural, optical, magnetic, and enhanced antibacterial properties of hydrothermally synthesized Sm-incorporating α-MoO_3 2D-layered nanoplates, RSC Adv. **12** (2022) 34584–34600, doi: https://doi.org/10.1039/D2RA05304G.
28. *A. Panja, K. Ghosh*, 4-Hydroxybenzaldehyde derived Schiff base gelators: case of the sustainability or rupturing of imine bonds towards the selective sensing of Ag^+ and Hg^{2+} ions via sol–gel methodology, New J. Chem. **43** (2019) 5139–5149, doi: https://doi.org/10.1039/C8NJ05056B.
29. *T. Vadivel, M. Dhamodaran*, Synthesis, characterization and antibacterial studies of ruthenium(III) complexes derived from chitosan schiff base, Int. J. Biol. Macromol. **90** (2016) 44–52, doi: https://doi.org/10.1016/j.ijbiomac.2015.11.008.
30. *R. Farhoosh, S. Johnny, M. Asnaashari, N. Molaahmadibahraseman, A. Sharif*, Structure–antioxidant activity relationships of *o*-hydroxyl, *o*-methoxy, and alkyl ester derivatives of *p*-hydroxybenzoic acid, Food Chem. **194** (2016) 128–134, doi: https://doi.org/10.1016/j.foodchem.2015.08.003.
31. *S. Manjula, S. Khan, A. Syed*, 4-Aminoantipyrine as a new

electrophilic coupling reagent for spectrophotometric determination of iron(III) in water, industrial effluent and soil samples, Sci. Asia **33** (2007) 455–460, doi: https://doi.org/10.2306/scienceasia1513-1874.2007.33.455.

32. *S. Hadi Kadhim, Q. Abd-Alla*, Synthesis and characteristic study of Co(II), Ni(II) and Cu(II) complexes of new Schiff base derived from 4-aminoantipyrine, Int. J. Chem. Sci. **15** (2017) 107, doi: https://doi.org/10.13140/RG.2.2.19888.00002.
33. *Y. Bayeh, F. Mohammed, M. Gebrezgiabher, F. Elemo, M. Getachew, M. Thomas*, Synthesis, characterization and antibacterial activities of polydentate Schiff bases, based on salicylaldehyde, Adv. Biol. Chem. **10** (2020) 127–139, doi: https://doi.org/10.4236/abc.2020.105010.
34. *M. Dizdar, M. Maksimović, A. Topčagić, M. Avdić, D. Vidic*, Synthesis and bioactivity of 1-substituted tetrahydroisoquinolines derived from phenolic aldehydes, Org. Commun. **16** (2023) 197–203, doi: https://doi.org/10.25135/acg.oc.159.2310.2920.
35. *S. C. Peitzika, E. Pontiki*, A review on recent approaches on molecular docking studies of novel compounds targeting acetylcholinesterase in Alzheimer disease, Molecules **28** (2023) 1084, doi: https://doi.org/10.3390/molecules28031084.
36. *P. Taslimi, F. Türkan, A. Cetin, H. Burhan, M. Karaman, I. Bildirici, İ. Gulçin, F. Şen*, Pyrazole[3,4-d]pyridazine derivatives: Molecular docking and explore of acetylcholinesterase and carbonic anhydrase enzymes inhibitors as anticholinergics potentials, Bioorg. Chem. **92** (2019) 103213, doi: https://doi.org/10.1016/j.bioorg.2019.103213.
37. *S. Sari, M. Yilmaz*, Synthesis, characterization, acetylcholinesterase inhibition, and molecular docking studies of new piperazine substituted dihydrofuran compounds, Med. Chem. Res. **29** (2020) 1804–1818, doi: https://doi.org/10.1007/s00044-020-02599-0.

SUPPLEMENTARY INFORMATION

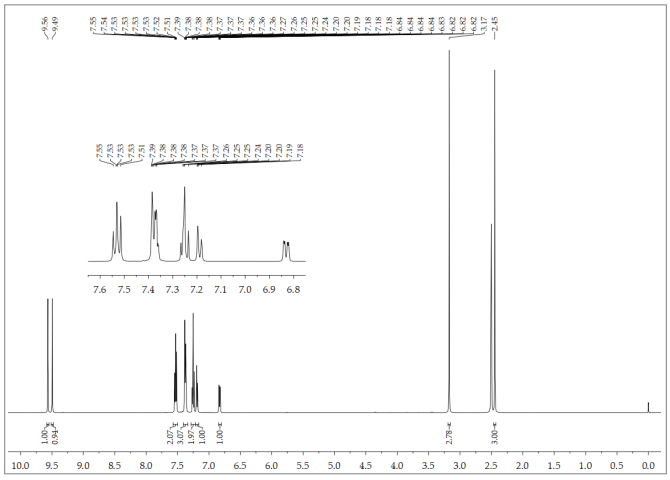

Fig. S1 – ^{1}H NMR spectrum of **1**

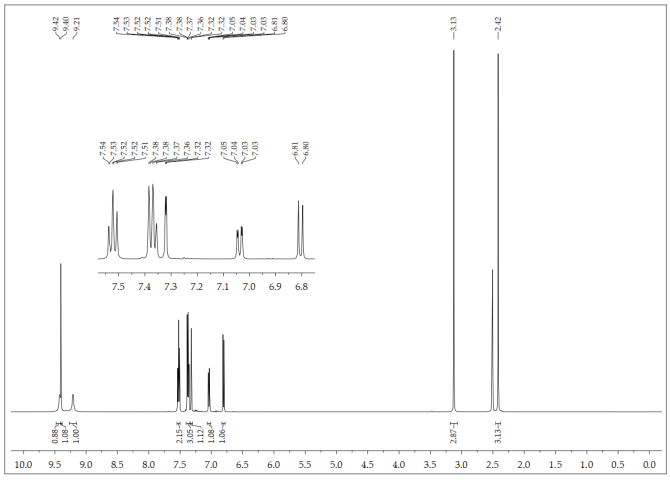

Fig. S3 – ^{1}H NMR spectrum of **3**

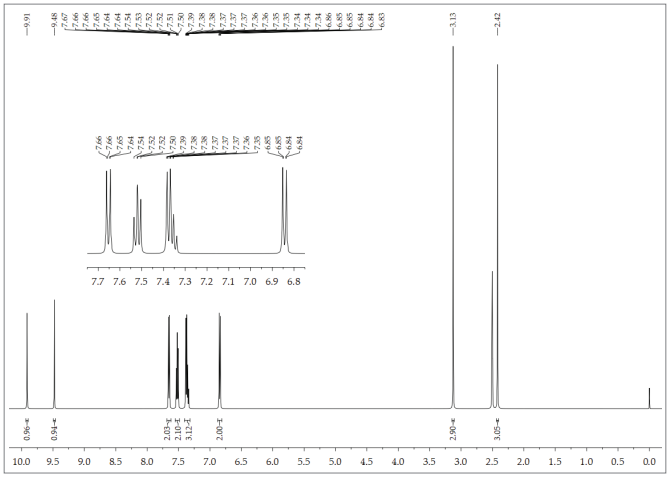

Fig. S2 – ^{1}H NMR spectrum of **2**

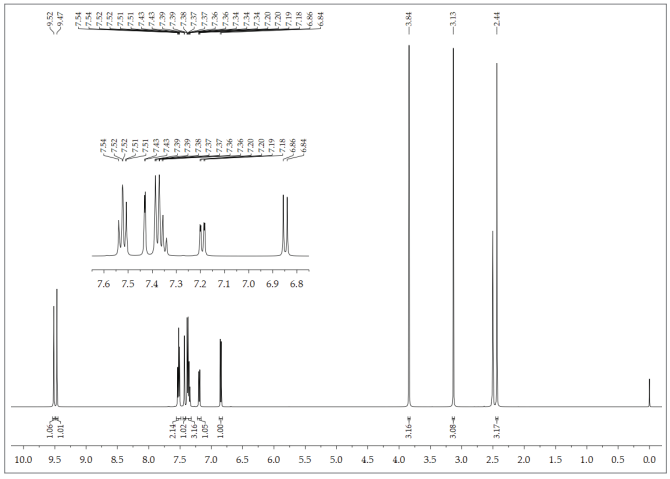

Fig. S4 – ^{1}H NMR spectrum of **4**

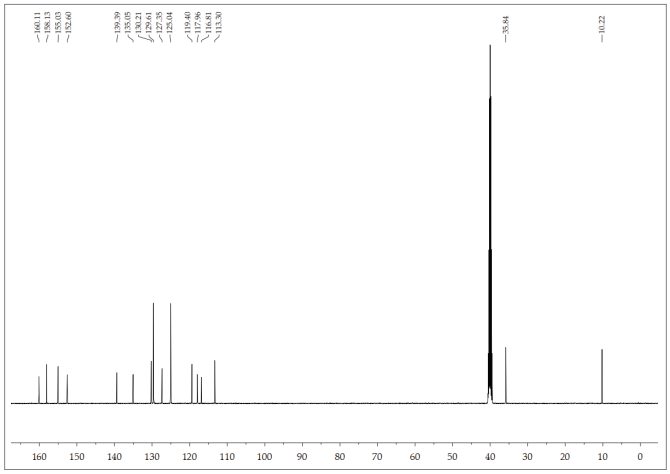

Fig. S5 – ^{13}C NMR spectrum of **1**

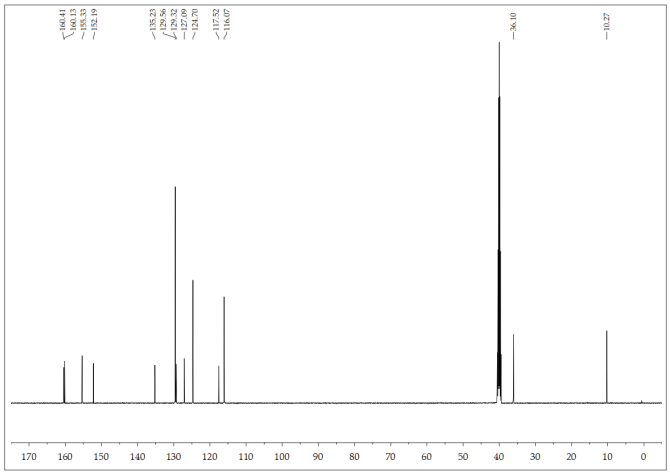

Fig. S6 – ^{13}C NMR spectrum of **2**

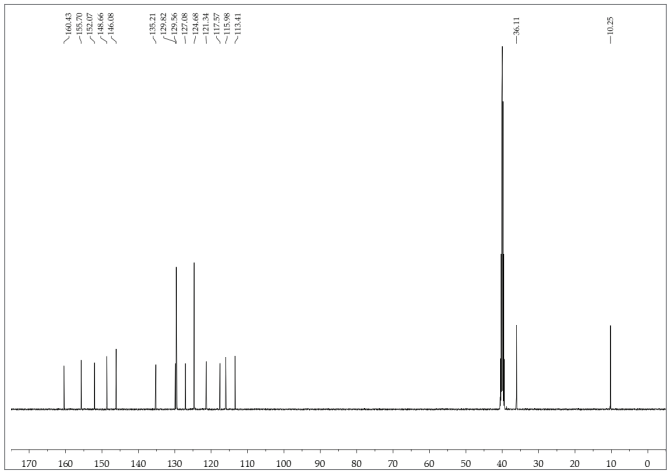

Fig. S7 – ^{13}C NMR spectrum of **3**

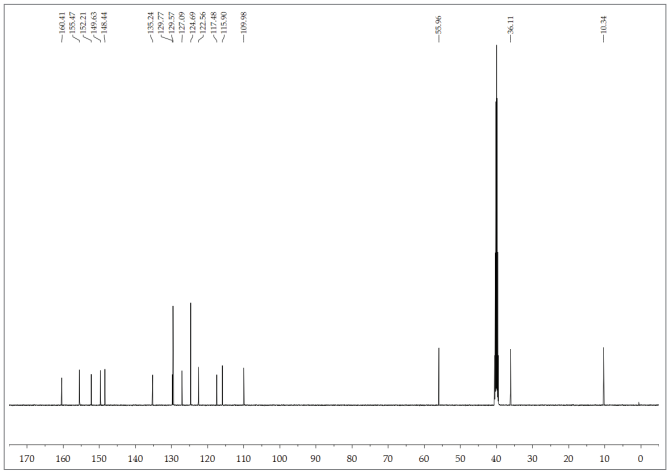

Fig. S8 – ^{13}C NMR spectrum of **4**

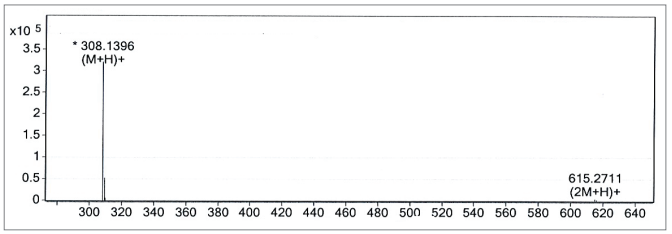

Fig. S9 – HR-ESI-MS spectrum of **1**

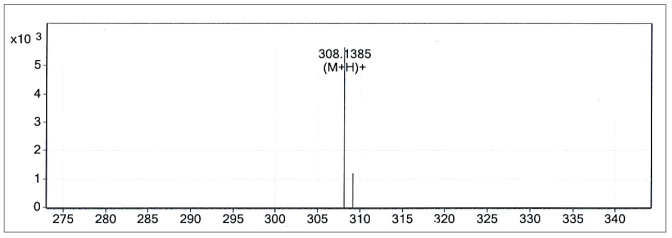

Fig. S10 – S10: HR-ESI-MS spectrum of **2**

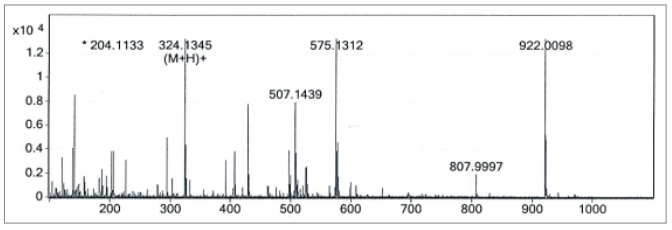

Fig. S11 – HR-ESI-MS spectrum of **3**

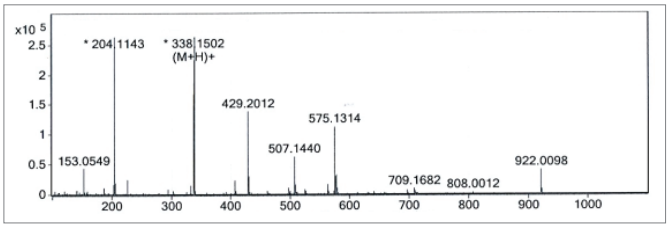

Fig. S12 – HR-ESI-MS spectrum of **4**

SAŽETAK

Sinteza i strukturni uvid u bioaktivnost imina s 1,5-dimetil-2-fenil-1*H*-pirazol-3(2*H*)-onom strukturnom jedinicom izvedenom iz fenolnih aldehida

Muamer Dizdar,[a*] *Anela Topčagić*,[a] *Monia Avdić*,[b] *Danijela Vidic* [a] i *Milka Maksimović* [a]

Istraživanje je usmjereno na sintezu, karakterizaciju i evaluaciju bioaktivnosti četiriju imina, dobivenih kondenzacijom 4-aminoantipirina s različitim fenolnim aldehidima: 3-hidroksibenzaldehidom, 4-hidroksibenzaldehidom, 3,4-dihidroksibenzaldehidom i 4-hidroksi-3-metoksibenzaldehidom. Ti su spojevi sintetizirani da bi se istražio njihov potencijal u različitim biološkim aktivnostima, uključujući antioksidativnu aktivnost, inhibitornu aktivnost na acetilkolinesterazu (AChE) i antibakterijsku aktivnost. Karakterizacija ovih imina pomoću IR, ^{1}H i ^{13}C NMR, HR-ESI-MS i elementarne analize potvrdila je njihove predložene strukture. Antioksidativna aktivnost sintetiziranih spojeva procijenjena je primjenjujući pet različitih metoda. Imin dobiven iz 3,4-dihidroksibenzaldehida pokazao je najvišu antioksidativnu aktivnost, što je pripisano njegovom kateholnom rasporedu fenolnih skupina. Nadalje, istražena je AChE-inhibitorna aktivnost ovih spojeva, otkrivajući da stupanj hidroksilacije i uvođenje metoksi skupine značajno utječu na njihovu inhibitornu učinkovitost. Studije molekulskog uklapanja istaknule su glavne interakcije između imina i AChE, identificirajući energetski najpovoljnija mjesta vezanja. Rezultati *in vitro* antibakterijske aktivnosti protiv kultura *Staphylococcus aureus*, meticilin-rezistentnog *Staphylococcus aureus*, *Pseudomonas aeruginosa* i *Escherichia coli* pokazali su široku aktivnost svih sintetiziranih spojeva. Ova sveobuhvatna analiza pokazala je značajan potencijal četiriju sintetiziranih imina kao bioaktivnih molekula, pružajući uvide u to kako strukturalne modifikacije mogu poboljšati njihove biološke funkcije.

Ključne riječi
*Sinteza, 1*H*-pirazol-3(2*H*)-on, fenolni aldehidi, in vitro bioaktivnost, in silico studija*

[a] *Prirodno-matematički fakultet Univerzitet u Sarajevu, Zmaja od Bosne 33–35, 71 000 Sarajevo, Bosna i Hercegovina*
[b] *Zavod za genetiku i bioinženjering, Internacionalni Burč univerzitet, Francuske revolucije bb, 71 210 Ilidža, Bosna i Hercegovina*

Izvorni znanstveni rad
Prispjelo 18. travnja 2024.
Prihvaćeno 3. lipnja 2024.